TURBULENT COMBUSTION IN THE LIGHT OF DIRECT AND LARGE EDDY SIMULATION

Luc Vervisch, Pascale Domingo and Raphael Hauguel
INSA de Rouen and UMR-CNRS-6614-CORIA,
Campus du Madrillet, BP 8,
F76801 Saint Etienne du Rouvray Cedex, France
vervisch@coria.fr, domingo@coria.fr,hauguel@coria.fr

INTRODUCTION

Modern societies rely on energy production that mainly results from combustion. As a drawback, the oxidation of hydrocarbon causes pollution and environmental problems that make accurate control of turbulent combustion a necessity. The progress in the design of combustion systems relies on the ability to perform subtle adjustments of their control parameters. This implies a precise knowledge of global turbulent combustion properties (residence time of the gases, local flame related features like turbulent mixing properties) and relies on information concerning the injection device that strongly impacts on flame stability and flame length. With recent progress in computer science and turbulence simulation, a non-negligible part of the improvement procedure of industrial combustion systems is now carried out in the light of numerical modeling. In the last decade, considerable data have been generated to understand premixed and nonpremixed turbulent combustion. They were obtained using a wide range of experimental and numerical techniques that are useful to improve combustion sub-models.

Turbulent combustion modeling motivates questions that may be addressed using Direct Numerical Simulation (DNS), where all the scales of the problem are fully resolved, at least in terms of scalar and velocity fluctuations, and where the chemical kinetics is often reduced (Givi, 1989; Poinsot, 1996; Vervisch and Poinsot, 1998). Accurate modeling cannot be rationally developed for a phenomenon whose behavior is not well known and this is where DNS is the most useful. For a long time, DNS has been restricted to very low Reynolds number flows. Today, the status of DNS is progressively evolving with the speed-up of computers and direct numerical simulations of laboratory jet-flame experiments have even been reported with realistic chemical kinetics (Mizobuchi et al., 2002).

In the next section, DNS of a premixed turbulent V-flame anchored on a hot wire is discussed. To allow for a reliable examination of the interaction between velocity fluctuations, acoustics and combustion, a novel numerical procedure is used in which a spectral solution of the Navier-Stokes equations is directly coupled to a high-order finite difference fully compressible DNS solver (sixth order PADE) (Lele, 1992). Using this combination of high-order solvers with a set of accurate boundary conditions, simulations have been performed where a premixed turbulent V-shape flame develops in grid turbulence. The chemistry is described with tabulated fully detailed kinetics. Flames are then analyzed in a turbulence featuring constant mean properties at any given streamwise position. The DNS is probed to propose a closure for premixed turbulent combustion, in which the FPI (Flame Prolongation of Intrinsic low Dimensional Manifold) chemistry tabulation is introduced (Gicquel et al., 2000).

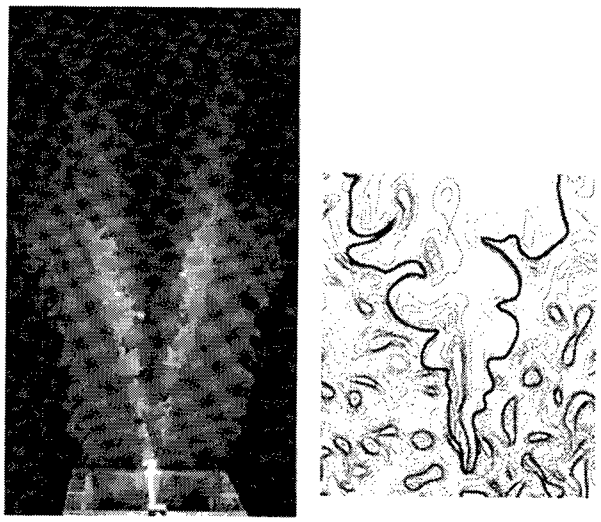

Figure 1: V-Flame. Left: experiment (Renou and Boukhalfa, 2003). Right: Direct Numerical Simulation

The second section discusses the possibilities of performing Large Eddy Simulation (LES) of partially premixed combustion. In nonpremixed combustion devices, unsteady large scales structures, which result from the rolling up of the shear layers, lead to incomplete mixing of the reactants. Then, the micromixing mechanism acting at smaller scale interacts with thin reaction zones, where heat and combustion products are released. When the unsteady large scale mixing is fully resolved, the information collected at the known scales may be of great help to model any unknown subgrid contribution. This is the objective of LES that simulates the large scale mixing process, which is mostly controlled by the geometry of the combustion chamber. If DNS is still limited to simplified flows, LES has reached a stage where it is useful for studying the flows in complex systems (Moin, 2002; Blin et al., 2003) and it now appears as a unique tool to tackle laboratory flames and real size combustion chambers where effects of unsteadiness play a crucial role (Colin et al., 2000; Pitsch and Steiner, 2000).

When fuel and oxidizer are injected separately, they can mix upstream of the flame zone, the flame then develops in partially premixed mixtures. Sometimes mixing is also organized with products to favour flame stabilization. This point is discussed in the second section where a procedure is reported that incorporates fundamental properties of partially premixed flames in a combustion sub-grid LES closure. The subgrid model takes advantage of the topology of the scalar field that is known at the resolved scales (Domingo et al.,

2002).

PREMIXED TURBULENT V-FLAME

Flow configuration, flame parameters and DNS numerical procedure

A V-shape flame may easily be obtained by introducing a hot wire in a stream of fully premixed reactants. The energy released by the wire initiates combustion and the resulting very localized burning kernel serves to stabilize a premixed flame that develops further downstream. In a laminar flow, the reaction layer propagates against the incoming fluid and a premixed V-shape flame is observed. When the flow is turbulent, the two wings of the flame are wrinkled by velocity fluctuations and a turbulent flame having a V-shape, in mean, is observed, as in fig. 1-left where an instantaneous flame front and a picture of the mean flame are combined from an experimental set-up (Renou and Boukhalfa, 2003). This configuration is of interest because grid turbulence may easily be generated in the incoming flow, so that combustion develops in a well characterized spatially decaying turbulence. Recent progress makes it possible to consider this configuration with DNS.

So far, fully compressible combustion DNS was restricted to turbulence that was freely decaying in time. This limitation was the result of difficulties encountered with flow activation techniques in order to capture, with accuracy, the strong coupling between pressure waves and flames. A low Mach number formalism is avoided because the DNS databases are also probed to study flame acoustics. Specifically for subsonic combustion, the use of any forcing based on a synthetic random phase generates spurious pressure oscillations that strongly perturb the flame behavior. To overcome this difficulty, two separate Navier Stokes solvers are combined so that the incoming grid-turbulence is exactly simulated in time (Guichard et al., 2001). A DNS spectral solver and a finite difference spatial solver evolve simultaneously in time. The spectral solution is used to generate a forced synthetic grid-turbulence that continuously enters the finite difference domain, with a galilean transformation applied to ensure the coupling between the solvers. Figure 3a shows the computational domains, on the left, the turbulence is forced in the spectral solution, on the right, a premixed turbulent V-flame develops in the spatially freely decaying turbulence. The forced turbulence entering the domain is thus a solution of the Navier Stokes equations.

To accurately compute the pressure field, the NSCBC boundary conditions (Poinsot and Lele, 1992) have been coupled with the forced turbulence. The time derivative of the velocity field is explicitly introduced in the calculation of the amplitude of the acoustic waves entering the domain. The flame-turbulence interaction is not affected by the forcing scheme and local weak pressure waves resulting from the formation of pockets of fresh gases traveling in the burnt gases are observed in fig. 2. The local pressure drops expected in the zone bordering egde-flames are also well captured. Two representative simulations have been performed where the integral turbulence scale is 10 times the characteristic flame thickness. In case (a), the ratio between the characteristic velocity fluctuations and the laminar flame speed is of the order of 1.25, while it is of the order of 2.5 in case (b). The velocity ratio is representative of values measured in V-flame experiments, but the ratio of length scale is an order of magnitude smaller than the one found in those experiments. The preliminary simulations reported here are two-dimensional, the forced turbulence is computed on a 512x512 mesh (spectral), while the flame requires a 1024x1024 grid for case (a) and 1024x2048 in case (b) (finite difference). Two-dimensionality is an oversimplification that may alter some of the results. Nevertheless, it was shown that most features of premixed flame turbulence interaction are found in two-dimensional DNS, as a result of the typical behavior of flame surfaces when they interact with vorticity (Poinsot and Veynante, 2001).

A variety of methods are now available to account for complex chemistry in numerical simulations (Lindstedt, 1998) and some DNS have even been realized incorporating fully detailed chemical kinetics and complex transport properties (Haworth et al., 2000; Im and Chen, 2002; Hilbert and Thévenin, 2002). Among the various methods for reducing the complexity of chemistry, one of them, ILDM (Intrinsic Low Dimensional Manifold) (Maas and Pope, 1992), is grounded on a direct analysis of the dynamic behavior of chemical systems. Relevant subspaces are determined by distinguishing between species linked to fast and slow time scales. Other techniques, like ISAT (Pope, 1997), are based on in-situ generation of look-up tables, which are constructed from the direct solving of the time evolution of the species concentrations. To overcome some limitations of ILMD, appearing when the number of control parameters needs to be highly reduced, the FPI (Flame Prolongation of ILMD) or FGM (Flamelet Generated Manifold) technique was recently proposed (Gicquel et al., 2000; van Oijen et al., 2001). FPI was shown to be attractive for capturing the low temperature region of premixed flames, by avoiding in ILMD the use of linear prolongation in the preheat zone that develops ahead of the thin reaction layer. For a given equivalence ratio of the mixture, FPI consists of tabulating the response of chemical species and temperature from the calculations of a laminar premixed flame, all the concentrations are then related to a unique progress variable. This chemistry tabulation was in fact anticipated in RANS (Reynolds Average Navier Stokes) flamelet modeling of premixed turbulent combustion, where the use of a burning rate tabulated from premixed laminar flames was introduced and then extended to nonpremixed turbulent combustion (Bradley et al., 1998).

For the stoichiometric V-flame simulations, the detailed methane-air GRI mechanism (Bowman et al., 1997) is retained to construct the FPI table. The burning rate of CO_2 and temperature are given in fig. 3c. The simulation of fig. 2 was performed using a single-step kinetics, to compare with detailed chemistry.

DNS to help modeling premixed turbulent combustion with complex chemistry and propagating flamelet

Figure 4 shows streamwise profiles of $\widetilde{c} = \overline{\rho c}/\overline{\rho}$, the Favre average of the progress variable, for various y transverse positions. Mean fields of relevant quantities are obtained after averaging the DNS data in time at every flow locations. Flame units are used in the graphs, then all quantities are normalized from the burning velocity and the characteristic thickness of a reference unstrained and planar laminar FPI premixed flame. The origin of the coordinates is located at the wire. For transverse distributions that are close to the centerline, fully burnt products ($\widetilde{c} = 1$) are reached at a streamwise position $x = 100$. The V-shape of the flame is recovered in fig. 4(a), since lower values of $\widetilde{c}$ are observed when the streamwise distribution is taken along a line further away from the wire. The influence of the increased turbulence in-

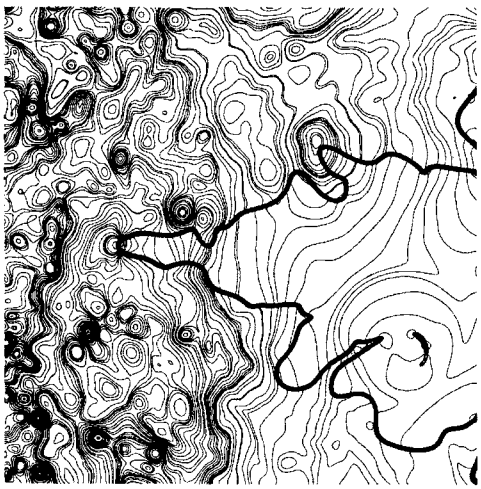

Figure 2: Pressure field (line) and reaction rate (bold), case (b).

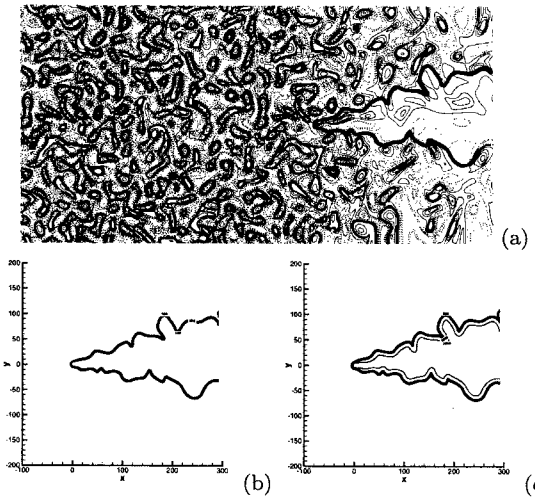

Figure 3: Snapshots of methane-air V-flame simulated with FPI tabulated GRI chemical mechanism, the turbulence intensity is $k^{1/2}/S_l^0 = 1.25$. (a) vorticity (line: positive) (dash: negative) and reaction rate (bold). (b) Reaction rate of CO_2 in s^{-1}. (c) Temperature in K.

tensity is visible in fig. 4(b), where some fresh gases are still mixed with burnt products at $x = 300$, even close to the centerline and $\widetilde{c}$ reaches unity much further downstream of the origin.

The chemical reactions occur at the dissipative scales of the turbulent motion, where molecular diffusion is acting to bring species into contact. Therefore both LES and RANS face the same difficulty: The unresolved small scale diffusion needs to be modeled and it is of fundamental importance for estimating the mean, or the subgrid, burning rate. When D is a representative diffusion coefficient, a characteristic mixing speed may be defined as $V_d = D|\nabla c|$. It is a measure of the speed at which the information diffuses across the local flame front of thickness $l_d = |\nabla c|^{-1}$. The ratio $\chi_c = V_d/l_d = D|\nabla c|^2$ is a time scale, usually called scalar dissipation rate, whose average $\overline{\rho}\widetilde{\chi}_c = \overline{\rho D|\nabla c|^2}$ is the stumbling block of any turbulent combustion modeling approach (Veynante and Vervisch, 2002).

In the FPI context, where species mass fractions are

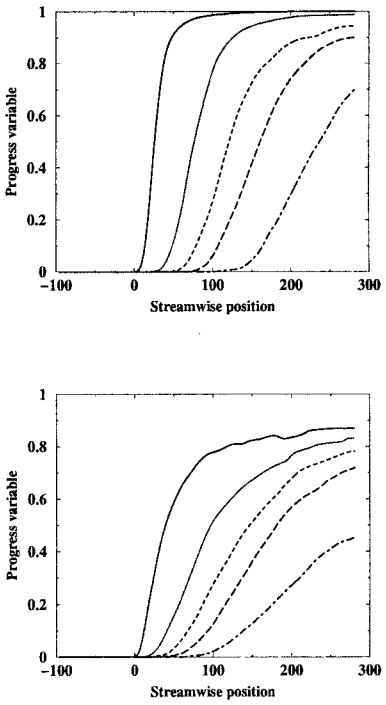

Figure 4: Streamwise distribution of, $\widetilde{c}$, Favre mean progress variable in case (a) and (b). Line: $y = 11.6$, Dotted line: $y = 23.6$, Dashed line: $y = 35.7$, Long dashed: $y = 47.7$, Dot-dashed: $y = 71.7$.

available in the form $Y_i(c)$, when the pdf (probability density function) of c is known, any mean quantity is then readily obtained:

$$\widetilde{Y}_i(\underline{x},t) = \int_c Y_i(c^*)\widetilde{P}(c^*;\underline{x},t)dc^* \qquad (1)$$

This relation is valid for both RANS and LES, in the latter, $\widetilde{P}(c^*)$ would denote a subgrid-pdf (Cook et al., 1997). This pdf may either be calculated or presumed, for instance via a beta-function. In both cases, turbulent micro-mixing mechanisms need to be estimated.

Basic closures for $\widetilde{\chi}_c$ may be obtained from an eddy-break up type hypothesis, then $\widetilde{\chi}_c = \widetilde{c''^2}/\tau_\chi$, with τ_χ a characteristic time scale that is usually estimated from a turbulence cascade time, $\tau_\chi = C_\chi \widetilde{k}/\widetilde{\epsilon}$, where $\widetilde{k}$ and $\widetilde{\epsilon}$ denote the kinetic turbulent energy and its dissipation rate. C_χ is a modeling constant. This linear relaxation is also sometimes generalized to the conditional value of diffusion, in the form of a LMSE or IEM micro-mixing modeling, widely used in pdf methods (Pope, 1985), then $\left(\overline{\nabla\cdot(\rho D\nabla c)|c^*}\right) \approx \overline{\rho}(\widetilde{c}-c^*)/\tau_\chi$. More elaborate closures exist, but to illustrate the difficulty of accounting for the impact of thin reaction zone gradient in micro-mixing modeling, a direct test of the simple closure $\widetilde{\chi}_c = C_\chi \widetilde{c''^2}/(\widetilde{k}/\widetilde{\epsilon})$ is proposed in fig. 5, where C_χ is set to unity. To reproduce the DNS data, it is seen that C_χ needs to vary not only from case (a) to case (b), therefore with the turbulence and flame characteristics, but also across the mean flame structure. In RANS, a first alternative consists of solving a balance equation for $\widetilde{\chi}_c$ (Mantel and Borghi, 1994).

This difficulty to estimate micro-scale diffusion is well documented in the literature and already observed in frozen flow mixing. In premixed combustion, molecular diffusion

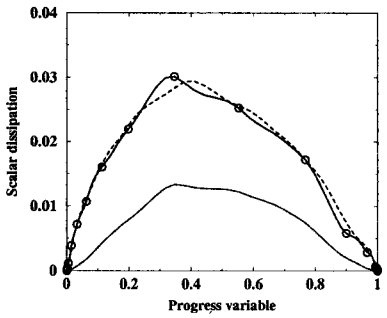

(a)

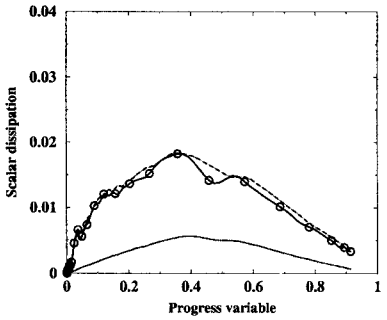

(b)

Figure 5: Transverse distribution at $x = 47.7$ of the scalar dissipation rate $\overline{\rho}\widetilde{\chi}_c$ plotted versus mean progress variable in case (a) and (b). Line with circle: DNS. Dotted line: $\widetilde{\chi}_c \approx \widetilde{c''^2}/(\widetilde{k}/\widetilde{\epsilon})$. Dashed line: Eq. 9

and chemical reaction are coupled to ensure flame propagation. Then, $\rho S_l(c)|\nabla c| = \nabla \cdot (\rho D \nabla c) + \dot{\omega}_c$, where $\dot{\omega}_c$ is the burning rate and $S_l(c)$ the relative progression velocity of the iso-c surfaces. In an unstrained and planar laminar flame, $S_l(c=0) = S_l^0$ is the so-called laminar flame burning velocity. Notice, however, that $S_l(c=0)$ may differ from S_l^0 because of strain and curvature.

To help in the modeling of premixed combustion, the physical decomposition of the scalar dissipation rate in characteristic speed and length may be recovered after introducing a gradient weighted, or surface, average: $\langle a \rangle_s = \overline{a|\nabla c|}/\overline{|\nabla c|}$ (Veynante and Vervisch, 2002). Then,

$$\overline{\rho}\widetilde{\chi}_c = \overline{\rho D |\nabla c|^2} = \langle \rho D |\nabla c| \rangle_s \, \overline{|\nabla c|} \tag{2}$$

The average turbulent speed of mixing thus appears in the form $\langle \rho D |\nabla c| \rangle_s$. The other contribution, $\overline{|\nabla c|}$, contains information on the wrinkling of the flame front. $\overline{|\nabla c|}$ is in fact the integral of the flame surface density function, $\Sigma(c^*) = \left(\overline{|\nabla c||c^*}\right) \overline{P}(c^*)$ (Vervisch et al., 1995), across the flame front:

$$\overline{|\nabla c|} = \int_c \Sigma(c^*) dc^* \tag{3}$$

$\overline{|\nabla c|}$ is a well known quantity that has been used in RANS and LES of premixed turbulent flames (Boger et al., 1998). The major advantage of Eq. 2 is to explicitly introduce a flame wrinkling length scale in the estimation of the scalar dissipation rate. Figure 6 displays streamwise profiles in the turbulent V-flame of $\overline{|\nabla c|}$ and of the wrinkling factor $\Xi = \overline{|\nabla c|}/|\overline{\nabla c}|$.

If the flame is able to promote propagation at the scale of the instantaneous thin interface between fresh and burnt gases, $\langle \rho D |\nabla c| \rangle_s$ is expected to be proportional to $\rho_o S_l^o$,

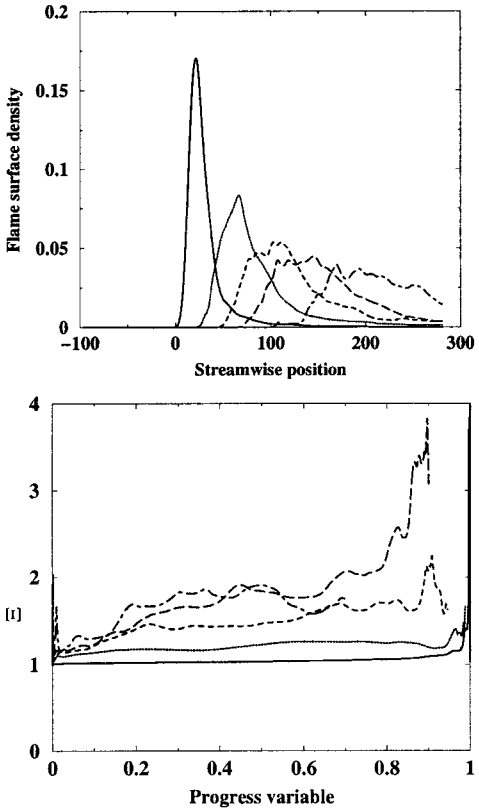

Figure 6: Streamwise distribution of generalized flame surface density $\overline{|\nabla c|}$ (top) and of the wrinkling factor Ξ (bottom), case (a). Line: $y = 11.6$, Dotted line: $y = 23.6$, Dashed line: $y = 35.7$, Long dashed: $y = 47.7$, Dot-dashed: $y = 71.7$.

where ρ_o is the density in the fresh gases. To seek out the exact form of $\langle \rho D |\nabla c| \rangle_s$, it is interesting to decompose the burning rate as:

$$\overline{\dot{\omega}}_c = \left\langle \frac{\dot{\omega}_c}{|\nabla c|} \right\rangle_s \overline{|\nabla c|} = \frac{\left\langle \frac{\dot{\omega}_c}{|\nabla c|} \right\rangle_s}{\langle \rho D |\nabla c| \rangle_s} \overline{\rho}\widetilde{\chi}_c \tag{4}$$

After integrating over thin reaction zones (Veynante and Vervisch, 2002), the BML analysis (Moss and Bray, 1977) is recovered and the ratio of surface averages of Eq. 4 is readily estimated:

$$\frac{\left\langle \frac{\dot{\omega}_c}{|\nabla c|} \right\rangle_s}{\langle \rho D |\nabla c| \rangle_s} = \frac{2}{2c_m - 1} \tag{5}$$

where

$$c_m = \frac{\int_c c^* \dot{\omega}_c(c^*) \overline{P}(c^*) dc^*}{\int_c \dot{\omega}_c(c^*) \overline{P}(c^*) dc^*} \tag{6}$$

Another estimation of the unknown burning rate may also be obtained from $\overline{|\nabla c|}$ (Boger et al., 1998):

$$\overline{\dot{\omega}}_c = \rho_o S_l^o \overline{|\nabla c|} \tag{7}$$

Combining Eq. 2 with Eq. 4, Eq. 5 and Eq. 7 leads to:

$$\langle \rho D |\nabla c| \rangle_s = \frac{1}{2}(2c_m - 1)\rho_o S_l^o \tag{8}$$

where $\langle \rho D |\nabla c| \rangle_s$ appears to depend on the laminar flame speed and on the impact of turbulence on the internal flame

structure via c_m. The scalar dissipation rate may then be expressed in the form:

$$\overline{\rho}\widetilde{\chi}_c = \overline{\rho D|\nabla c|^2} = \frac{1}{2}(2c_m - 1)\rho_o S_l^o \overline{|\nabla c|} \qquad (9)$$

This last expression combines a turbulent flame wrinkling length with the flame speed to estimate $\widetilde{\chi}_c$. It is tested in fig. 5 against the DNS results, when the c_m coefficient is calculated from Eq. 6 using a beta-pdf presumed from first and second order moment of the progress variable, the FPI tabulated chemistry provides $\dot{\omega}_c(c^*)$. An interesting agreement is observed between the approximated scalar dissipation rate and DNS. For those DNS, c_m stays close to its expected BML value, $c_m \approx 3/4$ (Moss and Bray, 1977).

These results suggest a simple closure associating pdf and flame surface density, in which the balance equations for the two first moments $\widetilde{c}$ and $\widetilde{c''^2}$ are considered to presume $\widetilde{P}(c^*)$. In those equations, the chemical sources, are obtained from FPI ($\dot{\omega}_c(c^*)$) and the pdf $\widetilde{P}(c^*)$:

$$\widetilde{\dot{\omega}}_c = \int_c \dot{\omega}_c(c^*)\widetilde{P}(c^*)dc^* \qquad (10)$$

$$\widetilde{c''\dot{\omega}_c} = \int_c (c^* - \widetilde{c})\dot{\omega}(c^*)\widetilde{P}(c^*)dc^* \qquad (11)$$

The scalar dissipation rate entering the equation for $\widetilde{c''^2}$ may then be calculated from Eq. 9, ensuring a coupling between propagating thin reaction zones and turbulent mixing. The transport equation for $\overline{|\nabla c|}$ has been the subject of many studies and closures are available in the literature for both RANS and LES (Poinsot and Veynante, 2001). LES of the real size three-dimensional V-flame experiments are under progress using this modeling approach. Flame parameters are then available at the resolved grid from Eq. 1.

LES OF PARTIALLY PREMIXED COMBUSTION

Introduction

The formal distinction between premixed and nonpremixed flames is relevant for characterizing the injection of reactants into the combustion chamber, nevertheless in nonpremixed systems, the flame developing further downstream may not exactly feature diffusion flame properties. For instance when fuel and oxidizer have been mixed at the molecular level before they can react. This straightforward observation has motivated further work, and fundamental properties of partially premixed flames are currently the subject of multiple studies. To help in the modeling of partially premixed turbulent combustion, it is intended below to propose and to test a LES procedure that combines premixed and diffusion flames.

With usual hydrocarbon fuel burning in air, the stoichiometric condition is located far on the air side. Therefore in terms of volume of fluid mixed, the amount of partially premixed rich mixture may dominate in practical combustion chambers and any information collected on partially premixed combustion may rapidly become of great interest. Various model problems have been used to investigate partially premixed combustion, they all reflect the large spectrum of combustion modes that can be observed in such flames.

Partially premixed combustion developing in counterflow flames has been investigated in various experiments, involving opposed-jets composed of more or less fuel rich and lean streams. By varying the equivalence ratio of the mixture, a flame stability map was drawn, which defines partially premixed methane-air opposed-jets flame existence (Lockett et al., 1999).

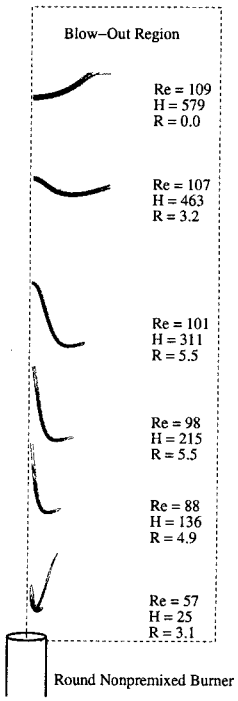

Figure 7: Lift-off simulations for different jet Reynolds numbers. Laminar flame bases are represented through their heat release rate. Re: Jet Reynolds number. H: Normalized lift-off height. R: Normalized radial position. Lengths are normalized using the burner radius.

Combining the combustion regimes may be helpful in reducing emissions of oxides of nitrogen from gas turbines. Along these lines, the fundamental properties of staged combustion has been studied by making use of sampling probe methods in laminar opposed-jet flames by varying the fuel side equivalence ratio (Li and Williams, 1999). A two stage flame with a green fuel-rich premixed flame and a blue diffusion flame with the maximum NO_x concentration near the blue flame were observed. Other careful measurements and scalar profiles of NO formation were reported in laminar opposed-flow partially premixed methane/air flames (Ravikrishna and Laurendeau, 2000; Barlow et al., 2001).

Axisymmetric co-flow is another configuration of interest for partially premixed combustion. In these co-flowing burners, the fuel and the surrounding secondary air are initially separated, as in a usual diffusion flame, but the fuel contains a given amount of primary air (Mcenally and Pfefferle, 2000). In the same context, six coflowing laminar methane/air and ethylene/air flames were studied by varying the equivalence ratio from infinity (nonpremixed) to 3 (Bennett et al., 2000; Bennett et al., 2001). Both experiments and detailed kinetics calculations have been carried out, where heat release profiles indicate the existence of an inner premixed and an outer nonpremixed flame front.

Partially premixed flames may also be investigated from turbulent laboratory jet-flames (Lee et al., 1997; Lee et al., 2000). A turbulent flame lifted on a round jet is a simplified configuration, recently reconsidered (Muñiz and Mungal,

1997; Maurey et al., 2000; Watson et al., 1999; Watson et al., 2000), where premixed combustion is observed in an initially fully nonpremixed system. Along a given iso-mixture fraction surface, a local premixed flame separates, at a given equivalence ratio, fresh and burnt gases in the vicinity of the lifted flame base. Over the range of mixture composition, the resulting collection of premixed flames may be connected in a partially premixed front that is eventually followed by a trailing diffusion flame.

The laminar archetype of such burning regime would be the so-called triple-flame or leading edge-flame (Phillips, 1965; Buckmaster and Weber, 1996; Dold, 1989; Daou and Liñán, 1998; Ghosal and Vervisch, 2000; Ghosal and Vervisch, 2001; Boulanger and Vervisch, 2002). Triple-flames have been studied using various tools. It was found that the speed of the triple-flame is controlled by two parameters: the curvature of the partially premixed front, determined by the rate of strain and gradient of mixture fraction imposed upon it, and the amount of heat released by combustion. Increasing the curvature reduces the flame speed. The effect of the heat release is the deflection of the flow upstream of the curved front, which has the net result of making the triple-flame propagate faster than S_l^o, the propagation speed of a fully premixed and planar stoichiometric flame. This flow deflection also induces a decrease of the mixture fraction gradient in the trailing diffusion flame (Ruetsch et al., 1995). The velocity of the overall triple flame structure is therefore greater than the premixed burning velocity, however, in a frame in which the triple flame is stationary, the flow slows down near the triple flame tip, to a velocity close to S_l^o. The flame base is thus expected to be in the vicinity of the point where the flow velocity, measured along the stoichiometric surface, is approximately the triple-flame velocity. Figure 7 shows DNS of laminar diffusion flames lifted on a round jet (Boulanger et al., 2003). Those simulations have revealed that the iso-S_l^o of the velocity field is strongly deflected by the burning zone, so that the flame can be stabilized closer to the burner than it would be without gas expansion. The flame is indeed stabilized in the simulations on the stoichiometric surface, at a point where the fluid velocity is close to the stoichiometric premixed flame burning velocity. However, the exact position of the stabilization point was found to be fully driven by heat release. The flow deflection resulting from heat release promotes an upstream movement in the cold flow of the point where the conditions of stabilization are encountered. This subtle iso-lines deviation is found to control flame stabilization. The flow deflection is more pronounced when the jet Reynolds number is increased. According to the numerical results, this derives from a strong modification of the structure of the simulated flame base depending on its downstream position. When the flame base moves downstream with the increase of fuel jet velocity, edge-flames or triple-flames with a burning trailing diffusion flame develop gradually into a large partially premixed front that deeply modifies the cold frozen flow mixing upstream of the burning zone (fig. 7) . Some of these effects may certainly persist at turbulent lifted flame bases.

The slot burner configuration was retained to analyze experimentally various partially premixed flames involving such triple- (Azzoni et al., 1999b) or inverse triple-flames (Aggarwal and Puri, 2001). The effects of gravity on triple-flames and the flame stretch effects on partially premixed flames were also considered with this burner (Azzoni et al., 1999a; Choi and Puri, 2000).

LES flame index $\overline{\xi}_p$ and turbulent lifted flames

Large Eddy Simulation appears as a good candidate to further analyze the behavior of partially premixed fronts.

LES applies a filter to the fields, so that only the contribution of the turbulent signal that can be resolved on a coarse grid is simulated. The filtering operation is expressed as:

$$\overline{q}(\underline{x},t) = \int_{-\infty}^{+\infty} q(\underline{x}^{'},t)G(\underline{x}-\underline{x}^{'})\,dx^{'} \qquad (12)$$

where $G(\underline{x}-\underline{x}^{'})$ is a normalized filter (Ferziger, 1993; Meneveau and Katz, 2000).

The main challenge in the modeling of partially premixed combustion is to achieve a dual description of varying premixed fronts (ie. defined for a non-uniform distribution of local equivalence ratios) and trailing diffusion flames. Premixed and diffusion turbulent combustion are two idealized regimes that are not antagonistic, but lead to flames with properties that are fundamentally different. The premixed front is thin and propagates combustion, the diffusion flame is more mixing controlled and does not propagate by itself, it is thus unlikely that a numerical model for diffusion flame can properly describe both regimes. This is especially true for the zone where combustion starts through the propagation of a thin front which can hardly be pictured as the ignition of a diffusive system.

When the fraction of fluid burning in either premixed or diffusion regime is determined, a straightforward modeling strategy may be obtained from the combination of robust combustion submodels, specifically organized for either premixed or diffusion flames. Any flame quantity would then be partitioned in a premixed and a nonpremixed contribution.

A flame indicator based on the scalar product of fuel and oxidizer normal vector may be introduced to distinguish, in the modeling, between premixed and nonpremixed flames (Yamashita et al., 1996). It was used to study partially premixed combustion during quenching and ignition of diffusion flames (Favier and Vervisch, 2001; Hilbert et al., 2001) and extended to LES of partially premixed combustion (Domingo et al., 2002). When studying diffusion flame quenching, it was found that the cross-scalar dissipation rate $\chi_{F,O} = -D\nabla Y_F \cdot \nabla Y_O$ is an interesting indicator of the combustion regime. F denotes the fuel and O is the oxidizer. $\chi_{F,O}$ may be organized as:

$$\chi_{F,O} = -D\nabla Y_F \cdot \nabla Y_O = -D|\nabla Y_F||\nabla Y_O|N_{F,O} \qquad (13)$$

where $N_{F,O} = \mathbf{n}_F \cdot \mathbf{n}_O$ is a cross-orientation factor with $\mathbf{n}_i = -\nabla Y_i/|\nabla Y_i|$ the normal vector to an iso-reactant surface. In diffusion flames, reactants are on both sides of the stoichiometric surface and $N_{F,O} < 0$ whereas in premixed flames, gradients of reactants are oriented towards the propagating front and $N_{F,O} > 0$ (Yamashita et al., 1996). This is illustrated in fig. 8 from measurements of the CH radical at the base of a turbulent lifted flames (Watson et al., 1999). An indicator of partial premixing ξ_p, or flame index, may then be written using Eq. 13:

$$\xi_p = \frac{1}{2}\left(N_{F,O}+1\right) = \frac{1}{2}\left(1 - \frac{\chi_{F,O}}{D|\nabla Y_F||\nabla Y_O|}\right) \qquad (14)$$

where $\xi_p = 1$ corresponds to fully premixed mixture and $\xi_p = 0$ to diffusion flamelets.

The orientation of the species vectors viewed from the resolved large eddies, $\overline{\mathbf{n}}_i^{\star}$, is directly indicated by the prod-

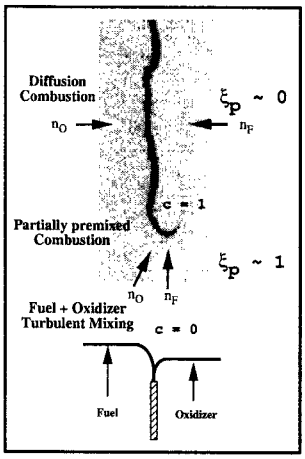

Figure 8: Instantaneous CH measurements (reaction zone) at the base of a turbulent lifted flame (Watson et al., 2000) are used to illustrate the studied model problem: Fuel and oxidizer are mixed prior to react in a partially premixed combustion mode. The thin partially premixed propagating front is followed by a trailing diffusion flame. The unit vectors $\mathbf{n}_O$ and $\mathbf{n}_F$ are normal to oxidizer and fuel isosurfaces respectively. The figure shows these unit vectors to be opposed to each other in the region of diffusion combustion, but almost fully aligned in the partially premixed combustion zone.

uct:[1]

$$\overline{\mathbf{n}}_F^\star \cdot \overline{\mathbf{n}}_O^\star = \nabla \overline{Y}_F \cdot \nabla \overline{Y}_O / |\nabla \overline{Y}_F||\nabla \overline{Y}_O| \qquad (15)$$

When the LES is weakly resolved, the determination of the combustion regime cannot be completed with information simply collected from the resolved scales. For instance $\overline{\mathbf{n}}_F^\star \cdot \overline{\mathbf{n}}_O^\star < 0$ indicating diffusion flames at the resolved eddies may need to be complemented by some partial premixing occurring at the subgrid level. The orientation of the species vectors may therefore change within the subgrid and the evaluation of the burning rate within the LES computational cell should account for this eventual subgrid reorientation that is followed by a change in the combustion regime.

The exact orientation factor $N_{F,O}$ is directly related to the cross-scalar dissipation rate $\chi_{F,O}$ (Eq. 13) that is representative of the mixing rate. $\chi_{F,O}$ is also linked to the flame index ξ_p (Eq. 14). The filtered cross-scalar dissipation rate is easily decomposed in resolved $\widetilde{\chi}^r_{F,O}$ and subgrid $\widetilde{\chi}^s_{F,O}$ parts:

$$\widetilde{\chi}_{F,O} = \widetilde{\chi}^r_{F,O} + \widetilde{\chi}^s_{F,O} \qquad (16)$$

where the resolved part may be written $\widetilde{\chi}^r_{F,O} = -D\nabla\widetilde{Y}_F \cdot \nabla\widetilde{Y}_O$. A closure for the subgrid part $\widetilde{\chi}^s_{F,O}$ was derived, leading to (Domingo et al., 2002):

$$\widetilde{\chi}_{F,O} \approx \widetilde{\chi}^r_{F,O} - Y_{F,o}Y_{O,o}\left(\overline{\mathcal{F}}_Z\widetilde{\chi}^s_c + \overline{\mathcal{F}}_c\widetilde{\chi}^s_Z\right) \qquad (17)$$

where $\overline{\rho}\widetilde{\chi}^s_Z$ and $\overline{\rho}\widetilde{\chi}^s_c$ are subgrid scalar dissipation rates. Z denotes the mixture fraction, a passive scalar equals to zero in pure oxidizer and to unity in pure air. $Y_{i,o}$ is a mass fraction measured in a feeding stream of the nonpremixed system. $\overline{\mathcal{F}}_c$ and $\overline{\mathcal{F}}_Z$ are fully determined filtered functions, which may be approximated using their resolved counterpart. The modeling issue is then again the determination of

[1] $\overline{\mathbf{n}}_i^\star = -\nabla\overline{Y}_i/|\nabla\overline{Y}_i|$ denotes the normal vector of the resolved field, that is different from $\overline{\mathbf{n}}_i = -\overline{\nabla Y_i/|\nabla Y_i|}$, the filtered value of the normal vector.

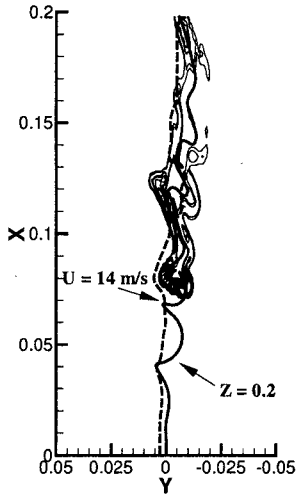

Figure 9: Isoline: heat release source term, thick line: stoichiometric line $Z = Z_s$, dashed line: velocity expressed as $U_s = U_{Ox}(1 - Z_s) + U_F Z_s$.

scalar dissipation rates, which may be achieved using developments similar to those presented in above section. Then, from Eq. 14, a modeled form may be proposed for the filtered flame index:

$$\overline{\xi}_p \approx \frac{1}{2}\left(1 - \frac{\widetilde{\chi}_{F,O}}{F_{norm}}\right) \qquad (18)$$

where F_{norm} is used to normalize $\widetilde{\chi}_{F,O} = \widetilde{\chi}^r_{F,O} + \widetilde{\chi}^s_{F,O}$, it may be written $F_{norm} = |\widetilde{\chi}^r_{F,O}| + |\widetilde{\chi}^s_{F,O}|$. This normalization ensures that $\overline{\xi}_p$ stays between zero and unity.

Any flame quantity may then be written:

$$\widetilde{Y}_i = \overline{\xi}_p\widetilde{Y}_i^p + (1 - \overline{\xi}_p)\widetilde{Y}_i^d \qquad (19)$$

where $\widetilde{Y}_i^p$ denotes the premixed contribution and $\widetilde{Y}_i^d$ the diffusion one.

LES of lifted flames

The behavior of lifted methane jet-flame is now reported when $\widetilde{Y}_i^p$ is obtained from a premixed LES approach based on a propagating progress variable (Boger and Veynante, 2000) and $\widetilde{Y}_i^d$ from diffusion flamelet modeling (Peters, 2000).

A fourth order finite volume skew-symmetric-like scheme is retained for the spatial derivatives (Ducros et al., 2000). This scheme was specifically developed and tested for LES, it is combined with a second order Runge Kutta explicit time stepping. The Lagrangian dynamic procedure determines the subgrid dissipative contribution (Meneveau et al., 1996).

Figure 9 is a two-dimensional snapshot of a lifted flame. The flames are stabilized within a turbulent cold wake. The maximum wake oxidizer velocity is $U_{Ox} = 10$ m/s, while the maximum fuel velocity is $U_F = 30$ m/s. The grid is organized so that at the flame base, the integral length eddies are of the order of the grid resolution.

A first point of interest is the exact location of the trailing diffusion flame. The flow velocity measured along the stoichiometric surface is a key quantity in lifted-flames, it is denoted U_s. An approximation of U_s may be writen,

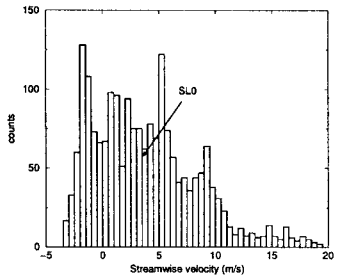

(a)

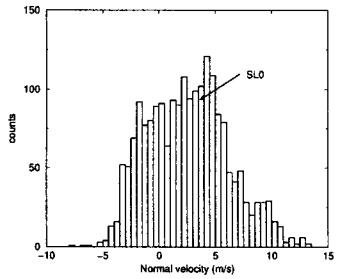

(b)

Figure 10: Velocity histograms collected at the edge-flame. (a): streamwise velocity $\tilde{u}_x$, (b) : normal velocity $\tilde{u}_n$.

$U_s \approx U_{Ox}(1 - Z_s) + U_F Z_s$ (Mungal, 2001), which is strictly valid for uniform pressure flow with a Schmidt number equal to unity and inlet velocity profiles featuring a top-hat shape. This simple correlation may be useful to locate the stoichiometric surface in experiments from the knowledge of the velocity field from PIV, by searching for the iso-U_s surface within the velocity distribution. The validity of this approximation is estimated from the simulations. Both the stoichiometric line $Z = Z_s$, determined from the resolved mixture fraction field, and the presumed iso-Z_s, obtained from the iso-U_s extracted from the resolved velocity field, are plotted in fig. (9). Due to the wake condition imposed at the inlet of the computational domain, a slight difference exists between the location of the U_s and Z_s isolines. Nevertheless, both lines stay quite close to each other in all the simulations, with a departure found at the leading edge flame (fig. 9). This departure is linked to a specific behavior of the flow velocity at the flame base and motivates below further discussion on the flow velocity at the location of the edge-flame.

Several competing theories have been proposed to explain the mechanism of partially premixed flame stabilization (Pitts, 1988). Recent experimental findings suggest that the flame is in fact composed of small edge-flames continuously interacting with the velocity fluctuations and propagating against the incoming flow (Muñiz and Mungal, 1997). However, the mean velocity measured at the flame base was found to be much larger than any triple-flame velocity (Schefer and Goix, 1998). LES fields may be analyzed to further understand the dynamics of the turbulent flame base.

To follow the properties of the stabilization zone, at every instant in time, the leading edge-flame is located as the point where the heat release is maximum. The direction of propagation of the edge-flame is known from $\mathbf{n} = -\nabla\overline{c}/|\nabla\overline{c}|$, the normal of the premixed flame front, which is estimated from the knowledge of the distribution of $\overline{c}$ in the vicinity of the edge-flame. Velocities are then collected at the leading edge of the flame. Velocity histograms presented in fig. 10 indicate that values higher than $10S_l^0$ are much less probable for the edge-flame normal velocity $\tilde{u}_n = -\tilde{\mathbf{u}} \cdot \mathbf{n}$ than for the streamwise velocity $\tilde{u}_x$. LES therefore shows that the leading edge-flame follows the low velocity region of the flow, of the order of S_l^0, but the edge-flame also adjusts itself so that the velocity in the direction normal to its local direction of propagation is as close as possible to the value S_l^0, when $\tilde{u}_n$ is measured in the vicinity of the maximum heat release. The same was also observed in experiment (Muñiz and Mungal, 1997; Maurey et al., 2000), where it is found that local and instantaneous edges of diffusion flames can take advantage of vorticity and micromixing to survive in a quite hostile environment, a behavior that was also found in DNS of triple flame vortices interaction (Favier and Vervisch, 1998).

These observations illustrate how Reynolds averaged values may not be the relevant quantities to fully understand turbulent flames. Numerics in turbulent combustion is a rapidly growing field and LES is likely to be most useful in a very near future.

ACKNOWLEDGMENTS

The simulations have been performed on the computers of IDRIS (Institut du Développement et des Ressources en Informatique Scientifique), CNRS. The constant support from Air Liquide, SNECMA, EC and Ministère de la Recherche is gratefully acknowledged. The authors have benefited from fruitful interactions with Dr. D. Veynante (Ecole Centrale Paris and CNRS) and Prof. K.N.C. Bray (Cambridge University).

REFERENCES

Aggarwal, S. K. and Puri, I. K. (2001). A numerical and experimental investigation of "inverse" triple flames. *Phys. Fluids*, 13(1):265–275.

Azzoni, R., Ratti, S., Puri, I. K., and Aggarwal, S. K. (1999a). Gravity effects on triple flames: flame structure and flow instability. *Phys. Fluids*, 11(11):3449–3464.

Azzoni, R., Ratti, S., Puri, I. K., and Aggarwal, S. K. (1999b). The structure of triple flames stabilized on a slot burner. *Combust. Flame*, 119(1/2):23–40.

Barlow, R. S., Karpetis, A. N., Frank, J. H., and Chen, J.-Y. (2001). Scalar profiles and no formation in laminar opposed-flow partially premixed methane/air flames. *Combust. Flame*, 127(3):2102–2118.

Bennett, B. A. V., S.Mcenally, C., Pfefferle, L. D., Smooke, M. D., and Colket, M. B. (2000). Computational and experimental study of axisymmetric coflow partially premixed methane/air flames. *Combust. Flame*, 123(4):522–546.

Bennett, B. A. V., S.Mcenally, C., Pfefferle, L. D., Smooke, M. D., and Colket, M. B. (2001). Computational and experimental study of axisymmetric coflow partially premixed ethylene/air flames. *Combust. Flame*, 127(1/2):2004–2022.

Blin, L., Hadjadj, A., and Vervisch, L. (2003). Large eddy simulation of turbulent flows in reversing systems. *J. of Turbulence*, 4(1):1–19.

Boger, M. and Veynante, D. (2000). Large eddy simulation of a turbulent premixed v-shaped flame. In Dopazo, C., editor, *Advances in Turbulence*, pages 449 – 452. CIMNE, BARCELONA, isbn: 84-89925-65-8 edition.

Boger, M., Veynante, D., Boughanem, H., and Trouvé, A. (1998). Direct numerical simulation analysis of flame surface density concept for large eddy simulation of turbulent premixed combustion. In *Twenty-seventh Symposium (Int.) on Combustion*, pages 917 – 925. The Combustion Institute.

Boulanger, J. and Vervisch, L. (2002). Diffusion edge-flame: Approximation of the flame tip damköhler number. *Combust. Flame*, 130(1):1–14.

Boulanger, J., Vervisch, L., Réveillon, J., and Ghosal, S. (2003). Effects of heat release in laminar diffusion flames lifted on round jets. *Combust. Flame*, Accepted, in press.

Bowman, C. T., Hanson, R. K., Gardiner, W. C., Lissianski, V., Frenklach, M., Goldenberg, M., Smith, G. P., Crosley, D. R., and Golden, D. M. (1997). An optimized detailed chemical reaction mechanism for methane combustion and no formation and reburning. Technical report, Gas Research Institute, Chicago, IL. Report No. GRI-97/0020.

Bradley, D., Gaskell, P. H., and Gu, X. J. (1998). The mathematical modeling of liftoff and blowoff of turbulent non-premixed methane jet flames at high strain rate. In *Twenty-Seventh Symposium (Int.) Symposium on combustion*, pages 1199–1206.

Buckmaster, J. and Weber, R. (1996). Edge-flame holding. In *Proceedings of the 26th Symp. (Int.) on Combustion.* The Combustion Institute, Pittsburgh.

Choi, C. W. and Puri, I. K. (2000). Flame stretch effetcs on partially premixed flames. *Combust. Flame*, 123(1/2):119–139.

Colin, O., Ducros, F., Veynante, D., and Poinsot, T. (2000). A thickened flame model for large eddy simulations of turbulent premixed combustion. *Physics of Fluids*, 12(7):1843–1863.

Cook, A. W., Riley, J. J., and Kosály, G. (1997). A laminar flamelet approach to subgrid-scale chemistry in turbulent flows. *Combust. Flame*, 109(3):332–341.

Daou, J. and Liñán, A. (1998). Triple flames in mixing layers with nonunity lewis numbers. *Proc. Combust. Inst.*, 27:667–674.

Dold, J. W. (1989). Flame propagation in a nonuniform mixture: analysis of a slowly varying triple flame. *Combust. Flame*, 76:71–88.

Domingo, P., Vervisch, L., and Bray, K. (2002). Partially premixed flamelets in les of nonpremixed turbulent combustion. *Combust. Theory and Modeling*, 6(4).

Ducros, F., Laporte, F., Soulères, T., Guinot, V., Moinat, P., and Caruelle, B. (2000). High-order fluxes for conservative skew-symmetric-like schemes in structured meshes: application to compressible flows. *J. Comput. Phys.*, 161:114–139.

Favier, V. and Vervisch, L. (1998). Effects of unsteadiness in edge-flames and liftoff in non-premixed turbulent combustion. *Proc. Combust. Inst.*, 28:1239–1245.

Favier, V. and Vervisch, L. (2001). Edge flames and partially premixed combustion in diffusion flame quenching. *Combust. Flame*, 125(1/2):788–803.

Ferziger, J. H. (1993). Subgrid scale modeling. In *Large eddy simulation of complex engineering and geophysical flows*, pages 37–54. Cambridge University Press.

Ghosal, S. and Vervisch, L. (2000). Theoretical and numerical investigation of symmetrical triple flame using a parabolic flame tip approximation. *J. Fluid Mech.*, 415:227–260.

Ghosal, S. and Vervisch, L. (2001). Stability diagram for liftoff and blowout of a round jet laminar diffusion flame. *Combust. Flame*, 124(4):646–655.

Gicquel, O., Darabiha, N., and Thevenin, D. (2000). Laminar premixed hydrogen / air counterflow flame simulations using flame prolongation of ildm with differential diffusion. *Proc. Comb. Inst.*, 28:1901–1908.

Givi, P. (1989). Model free simulations of turbulent reactive flows. *Prog. Energy Combust. Sci.*, 15:1–107.

Guichard, L., Réveillon, J., and Hauguel, R. (2001). A numerical procedure to stabilize planar turbulent premixed flames. In *Second International Symposium on Turbulence and Shear Flow Phenomena.*

Haworth, D., Cuenot, B., Poinsot, T., and Blint, R. (2000). Numerical simulation of turbulent propane-air combustion with non-homogeneous reactants. *Combust. Flame*, 121(3):395–417.

Hilbert, R. and Thévenin, D. (2002). Autoignition of turbulent non-premixed flames investigated using direct numerical simulations. *Combust Flame*, 128(1-2):22–37.

Hilbert, R., Thévenin, D., and Vervisch, L. (2001). Partially-premixed combustion during auto-ignition of a turbulent nonpremixed flame. In *Direct and Large-Eddy Simulation-IV,, Twente, July 28-20.*

Im, H. G. and Chen, J. H. (2002). Preferential diffusion effects on the burning rate of interacting turbulent premixed hydrogen-air flames. *Combust. Flame*, 131(3):246–258.

Lee, T.-W., Fenton, M., and Shankland, R. (1997). Effects of variable partial premixing on turbulent jet flame structure. *Combust. Flame*, 109(4):536–548.

Lee, T.-W., Mitovic, A., and Wang, T. (2000). Temperature, velocity, and nox/co emission measurements in turbulent flames: effects of partial premixing with central fuel injection. *Combust. Flame*, 121(1/2):378–385.

Lele, S. K. (1992). Compact finite difference schemes with spectral like resolution. *J. Comput. Phys.*, 103:16–42.

Li, S. C. and Williams, F. A. (1999). Nox formation in two-stage methane-air flames. *Combust. Flame*, 118(3):399–414.

Lindstedt, P. (1998). Modeling of the chemical complexities of flames. *Proc. Comb. Inst.*, 27:269–285.

Lockett, R. D., Boulanger, B., Harding, S., and Greenhalgh, D. A. (1999). The structure and stability of the laminar counter-flow partially premixed methane/air triple flame. *Combust. Flame*, 119(1/2):109–120.

Maas, U. and Pope, S. (1992). Simplifying chemical kinetics: Intrinsic low-dimensional manifolds in composition space. *Combust. Flame*, 88:239–264.

Mantel, T. and Borghi, R. (1994). A new model of premixed wrinkled flame propagation based on a scalar dissipation equation. *Combust. Flame*, 96(4).

Maurey, C., Cessou, A., and Stepowski, D. (2000). Statistical flow dynamic properties conditioned on the oscillating stabilization location of turbulent lifted flame. *Proc. Combust. Inst.*, 28:545–551.

Mcenally, C. S. and Pfefferle, L. D. (2000). Experimental study of nonfuel hydrocarbons and soot in coflowing partially premixed ethylene/air flames. *Combust. Flame*, 121(4):575–592.

Meneveau, C. and Katz, J. (2000). Scale invariance and turbulence models for large-eddy simulation. *Annual Review of Fluid Mechanics*, 32:1–32.

Meneveau, C., Lund, T. S., and Cabot, W. (1996). A lagrangian dynamic subgrid-scale model of turbulence. *J. Fluid Mech.*, pages 353–386.

Mizobuchi, Y., Tachibana, S., Shinjo, J., Ogawa, S., and Takeno, T. (2002). A numerical analysis on structure of turbulent hydrogen jet lifted flame. *Proc Combust Inst*, 29.

Moin, P. (2002). Advances in large eddy simulation methodology for complex flows. *Int. J. Heat Fluid Flow*, 23(6):710–720.

Moss, J.-B. and Bray, K. (1977). A unified statistical model of the premixed turbulent flame. *Acta Astronaut.*, 4:291–319.

Muñiz, L. and Mungal, M. G. (1997). Instantaneous flame-stabilization velocities in lifted-jet diffusion flames. *Combust. Flame*, 111(1/2):16–31.

Mungal, M. G. (2001). Experiments in combustion. In Beeck, J. V., Vervisch, L., and Veynante, D., editors, *Turbulence and Combustion*, pages 1–184. von Karman Institute for Fluid Dynamics.

Peters, N. (2000). *Turbulent Combustion.* Cambridge University Press.

Phillips, H. (1965). Flame in a buoyant methane layer. *Proc. Combust. Inst.*, 10:1277–1283.

Pitsch, H. and Steiner, H. (2000). Large-eddy simulation of a turbulent piloted methane/air diffusion flame (sandia flame d). *Physics of Fluids*, 12(10):2541–2554.

Pitts, W. (1988). Assesment of theories for the behavior and blowout of lifted turbulent jet diffusion flame. In *Proceedings of the 22nd Symposium (Int) on Combustion.* The Combustion Institute Pittsburgh.

Poinsot, T. (1996). Using direct numerical simulations to understand premixed turbulent combustion. In *Proceedings of the 26th Symp. (Int.) on Combustion. The Combustion Institute, Pittsburgh.*, pages 219–232.

Poinsot, T. and Lele, S. K. (1992). Boundary conditions for direct simulations of compressible viscous flows. *J. Comput. Phys.*, 1(101):104–129.

Poinsot, T. and Veynante, D. (2001). *Theoretical and Numerical Combustion.* R. T. Edwards, Inc.

Pope, S. B. (1985). Pdf method for turbulent reacting flows. *Prog. Energy Combust. Sci.*, 11:119–195.

Pope, S. B. (1997). Computationally efficient implementation of combustion chemistry using in situ adaptive tabulation. *Combust. Theory Modelling*, 1:41–63.

Ravikrishna, R. V. and Laurendeau, N. M. (2000). Laser-induced fluorescence measurements and modeling of nitric oxide in couterflow partially premixed flames. *Combust. Flame*, 122(4):474–482.

Renou, B. and Boukhalfa, M. (2003). Experimental analysis of a premixed turbulent v-flame. *Private communitation*, INSA de Rouen and CNRS-CORIA.

Ruetsch, G., Vervisch, L., and Liñán, A. (1995). Effects of heat release on triple flame. *Phys. Fluids*, 6(7):1447–1454.

Schefer, R. W. and Goix, P. (1998). Mechanism of flame stabilization in turbulent, lifted jet flames. *Combust. Flame*, 112(4):559–574.

van Oijen, J. A., Lammers, F. A., and de Goey, L. P. H. (2001). Modeling of complex premixed burner systems by using flamelet-generated manifolds. *Combust. Flame*, 127(3):2124–2134.

Vervisch, L., Bidaux, E., Bray, K. N. C., and Kollmann, W. (1995). Surface density function in premixed turbulent combustion modeling, similarities between probability density function and flame surface approaches. *Phys. Fluids*, 10(7):2496–2503.

Vervisch, L. and Poinsot, T. (1998). Direct numerical simulation of non-premixed turbulent flame. *Annu. Rev. Fluid Mech.*, 30:655–692.

Veynante, D. and Vervisch, L. (2002). Turbulent combustion modeling. *Prog Energy Combust Sci*, 28:193–266.

Watson, K. A., Lyons, K. M., Donbar, J. M., and Carter, C. D. (1999). Observations on the leading edge in lifted flame stabilization. *Combust. Flame*, 119(1/2):199–202.

Watson, K. A., Lyons, K. M., Donbar, J. M., and Carter, C. D. (2000). Simultaneous rayleigh imaging and ch-plif measurements in a lifted jet diffusion flame. *Combust. Flame*, 123(1/2):252–265.

Yamashita, H., Shimada, M., and Takeno, T. (1996). A numerical study on flame stability at the transition point of jet diffusion flames. *Proc. Combust. Inst*, 26:27–34.